Encapsulation and storage of therapeutic fibrin-homing peptides using conducting polymer nanoparticles for programmed release by electrical stimulation

Anna Puiggalí-Jou,[a,*] Luis J. del Valle[a] and Carlos Alemán[a,b,*]

[a] Departament d'Enginyeria Química and Barcelona Research Center for Multiscale Science and Engineering, EEBE, Universitat Politècnica de Catalunya, C/Eduard Maristany 10-14, Barcelona 08019, Spain

[b] Institute for Bioengineering of Catalonia (IBEC), The Barcelona Institute of Science and Technology, Baldiri Reixac 10-12, 08028 Barcelona, Spain

[*] Correspondence to: anna.puiggali@upc.edu and carlos.aleman@upc.edu

ABSTRACT

CREKA (Cys-Arg-Glu-Lys-Ala) is an important fibrin-homing pentapeptide that has been extensively demonstrated for diagnoses and therapies (*e.g.* image diagnosis of tumors and to inhibit tumor cell migration and invasion). Although CREKA-loaded nanoparticles (NPs) have received major interest as efficient biomedical systems for cancer diagnosis and treatment, almost no control on the peptide release has been achieved yet. Herein, we report the development of conductive polymer (CP) NPs as therapeutic CREKA carriers for controlled dose administration through electric stimuli. Furthermore, the study has been extended to CR(*N*Me)EKA (Scheme 1), a previously engineered CREKA analogue in which Glu was replaced by *N*-methyl-Glu for improvement of the peptide resistance against proteolysis, which is one of the major weaknesses of therapeutic peptide delivery, and for enhancement of the tumor homing capacity by over-stabilizing the bioactive conformation. Particularly, the present work has been focused on understanding the interactions between the newly designed nanoengineered materials and biological fluids and the achievement of a modulated peptide release by fine tuning the electrical *stimuli*. Two different types of stimuli were compared, chronoamperometry *vs* cyclic voltammetry, being the latter more effective.

Keywords: Controlled release; CREKA; drug delivery; electrical stimuli; PEDOT; Tumor homing peptide

INTRODUCTION

The fibrin-homing pentapeptide Cys-Arg-Glu-Lys-Ala (CREKA; Scheme 1) interacts with fibrin clots and possesses favorable targeting ability to fibrin-fibronectin complexes in animal models of neoplasia, atherosclerosis and myocardial ischemica-reperfusion.[1-3] Since this peptide was discovered by *in vivo* phage display technique,[4] it has been extensively utilized for the image diagnosis of tumors[5-9] and to inhibit tumor cell migration and invasion.[10,11] The fibrinogen released from tumor vessels is transformed into fibrin fibers by thrombin, which cleaves and removes fibrinopeptides. CREKA affects this process, catalyzing a very fast aggregation process, which results in a stepwise linear growth of fibrin meshes and particles.[3]

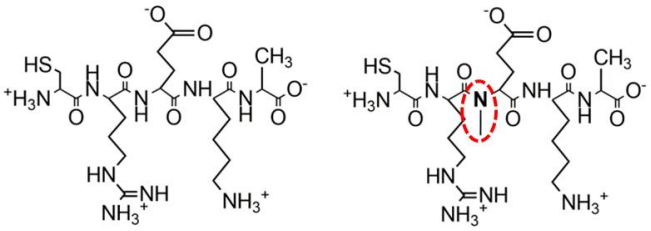

Scheme 1. Chemical structure of CREKA (left) and CR(*N*Me)EKA (right). The chemical modification introduced in the Glu residue is marked in red.

In order to improve the efficacy of CREKA-based diagnoses and therapies, most research has focused on loading this peptide in active targeting nanoparticles (NPs). For example, CREKA has been conjugated with polymer NPs[12-14] [*e.g.* poly(ethylene glycol) (PEG), PEG-polylactic acid and polyamidoamine dendrimers], polymer-metal and polymer-metal oxide hybrid NPs[15,16] [*e.g.* Au-PEG, Fe_2O_3-PEG and Fe_3O_4-poly(lactic-*co*-glycolic acid)], and inorganic NPs[11,17-19] (*e.g.* Fe_2O_3 and mesoporous silica) for targeted imaging of tumor cells and cancer therapies. Furthermore, this pentapeptide has been encapsulated in liposomes for anti-metastasis therapies against

breast cancer.[10] The successful results obtained in all cases should be attributed to high stability of the bioactive conformation,[20] which is preserved when the peptide is bound to NPs.[21,22]

In recent years, conducting polymers (CPs) have been considered as promising materials for the fabrication of electrically driven drug loading and delivery systems. Thus, CPs exhibit excellent redox properties that promote the uptake (oxidation) and expulsion (reduction) of charged drugs by applying an external electric field.[23-25] Because of the reversibility of their redox properties, CP-based systems provide not only on demand drug release, according to the clinical needs, but also repeatability of the delivered flux. Moreover, the potential of electro-responsive CP NPs has been recently extended to neutral drugs, such as curcumin, allowing their electrically pulsed linearly scalable, and on demand release.[26,27] Notably, although CREKA has been incorporated to CP films to promote its ability to bind fibrin-fibronectin complexes,[28,29] this pentapeptide has never been loaded in CP NPs to modulate and program its controlled release with the applied stimulus. Although the utilization of CPs as drug delivery systems for humans is still in its early stages,[30] *in vivo* assays using different types of electrochemical techniques for electrical stimulation have been successfully conducted.[31-33]

In an early work,[28] CREKA was entrapped into films of poly(3,4-ethylenethiophene) (PEDOT), which is one of the most studied CPs because of its excellent properties (*i.e.* electrical conductivity, electrochemical activity and biocompatibility and great stability of the properties when exposed to air),[34-38] using by applying different electrochemical procedures. The highest peptide concentration (*i.e.* one CREKA molecule per six repeat units) was obtained when PEDOT/CREKA films were prepared by chronoamperometry using a basic aqueous solution and adhered onto another previously generated PEDOT

film. Interestingly, PEDOT/CREKA films favored the cellular proliferation, which has been proved to be due to the binding of the peptide to the fibrin molecules from the serum used as a supplement in the culture media.[28] More recently, PEDOT/CREKA films were found to affect the fibrin thrombin-catalyzed polymerization, inducing a very fast aggregation process.[29] In absence of thrombin, PEDOT/CREKA induced a stepwise linear growth of fibrin particles.[29]

In this work we are not focused on the therapeutic applications of CREKA, which have been extensively discussed,[1-19,28,29] but on developing an electroactive bioplatform for storage and on-demand peptide release by electrical stimulation. For this purpose, PEDOT NPs obtained by emulsion polymerization have been loaded *in situ* with CREKA for electro-stimulated release. Furthermore, the study has been extended to CR(*N*Me)EKA (Scheme 1), a previously engineered CREKA analogue in which Glu was replaced by *N*-methyl-Glu for improvement of the peptide resistance against proteolysis and for enhancement of the tumor homing capacity by over-stabilizing the bioactive conformation.[11] Results strongly support that PEDOT NPs are promising sensitive and stable bioplatforms for the storage and administration of controlled doses of CREKA and CR(*N*Me)EKA through electric stimuli. This approach is smart, facile and has excellent control for potential medical applications in which CREKA is gaining interest.

RESULTS AND DISCUSSION

Characterization of peptide-loaded NPs

PEDOT NPs can be easily synthesized with the assistance of hard-templates[39-42] that *a priori* are expected to give better control on the size and colloidal stability than soft templates, as for example surfactants.[43] However, stable PEDOT NPs were recently

obtained using sodium dodecyl benzene sulfonate (SDBS) and iron (III) chloride as stabilizer and oxidant, respectively.[44,45] In this work, PEDOT NPs have been prepared in water using ammonium persulfate (APS) as oxidizing agent and dodecyl benzene sulfonic acid (DBSA) as both stabilizer and doping agent, as reported in previous work.[26] The two pentapeptides, CREKA and CR(*N*Me)EKA, were loaded *in situ* during the emulsion polymerization using the reaction conditions described in the Supporting Information. Hereafter, the resulting CREKA- and CR(*N*Me)EKA-loaded PEDOT NPs are denoted CREKA/PEDOT and CR(*N*Me)EKA/PEDOT, respectively.

The morphology of unloaded and peptide-loaded NPs is compared in Figure 1, which includes representative scanning electron microscopy (SEM) and transmission electron microscopy (TEM) micrographs, and atomic force microscopy (AFM). SEM micrographs (Figure 1a) show that the surface of the NPs is relatively smooth and uniform. Although the shape of unloaded NPs is relatively ill-defined, which has been attributed to the presence of surfactant left on the dried NPs, their sphericity increases when CREKA and CR(NMe)EKA are loaded. Thus, the drawback induced by the surfactant is partially compensated by the incorporation of charged peptides, which improves the spherical shape of the NPs. This feature is clearly evidenced when TEM micrographs recorded for isolated particles are compared with those obtained for CREKA/PEDOT and CR(NMe)EKA/PEDOT NPs (Figure 1b). The distribution histograms (Figure 1c) obtained by measuring the diameter of such isolated particles (n= 100 in all cases) indicate that the size increases as follows: PEDOT NPs (35 ± 6 nm) < CREKA/PEDOT NPs (43 ± 6 nm) < CR(*N*Me)EKA/PEDOT NPs (47 ± 9 nm). 3D topographic AFM images (Figure 1d) of isolated NPs show a surface smoothness similar to that displayed by SEM micrographs. Besides, height profiles (Figure 1e) confirm that the size of the NPs increases upon the loading of the peptides, even though,

due to the influence of the tip, the diameters are less precise when determined by AFM than by SEM.

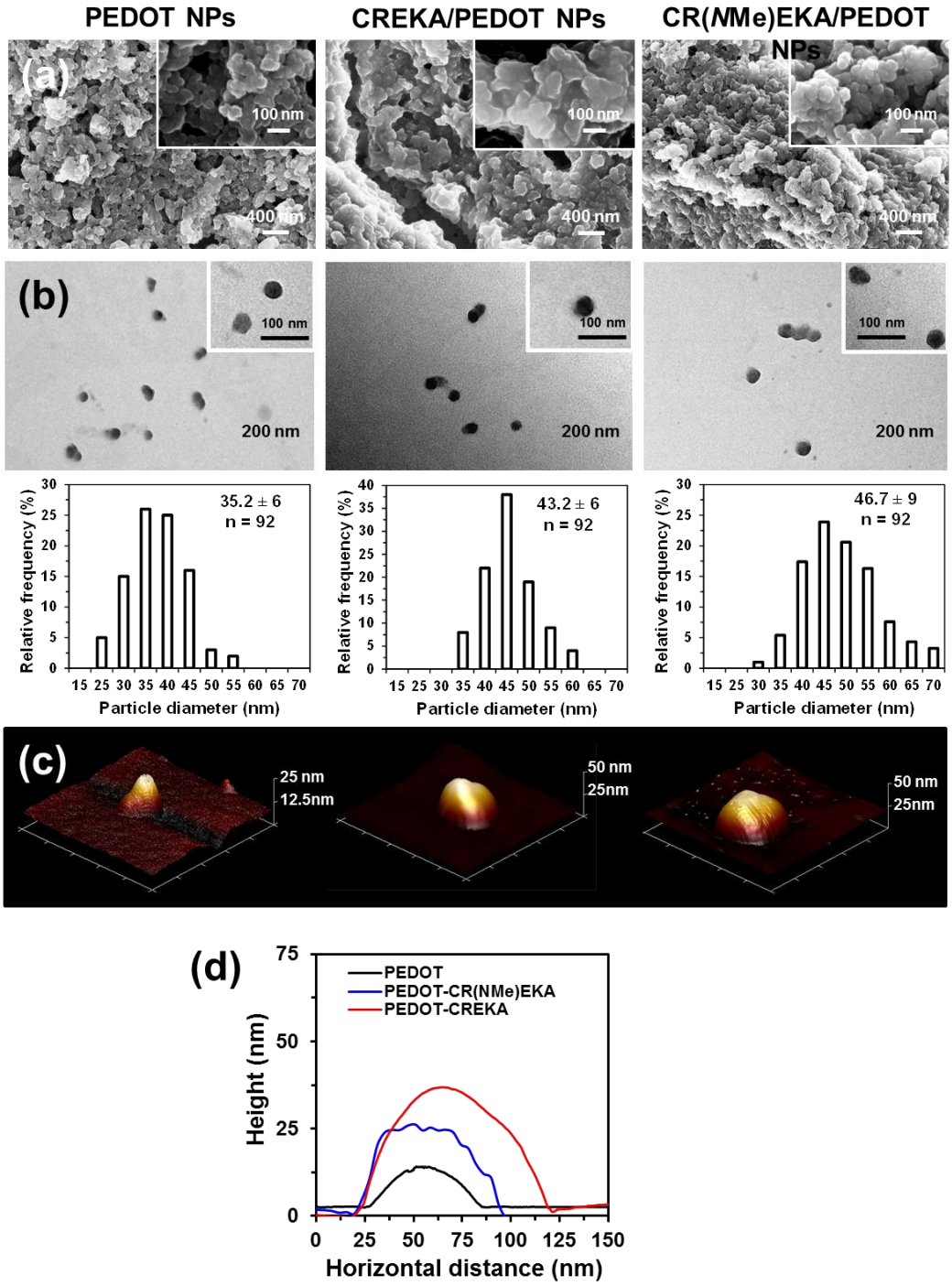

Figure 1. Morphological characterization of PEDOT, CREKA/PEDOT and CR(*N*Me)EKA/PEDOT NPs: representative (a) SEM, (b) TEM and (c) AFM images of NPs aggregates. The size histograms (n= 100) displayed in (b) were derived from TEM images of isolated NPs. (d) Height profiles for the isolated NPs displayed in (d).

Figure 2a compares the FTIR spectra of DBSA, PEDOT NPs and the two peptide/PEDOT NPs. The DBSA spectrum shows strong absorbance bands at 2922 and 2853 cm^{-1}, which are assigned to the aliphatic $–CH_2$ and $–CH_3$ stretching vibration modes, respectively, and at 1646 cm^{-1} that are attributed to the C=C stretching vibration band of the phenyl side group. The spectrum recorded for PEDOT NPs display characteristic bands that correspond to the C=C stretching at 1650 and 1472 cm^{-1}, the C–C of the quinoid thiophene ring at 1351 cm^{-1}, the C–O–C vibrations at 1218 and 1058 cm^{-1}, and the stretch of the C–S bond in the thiophene ring at 836 and 683 cm^{-1}. The presence of the shoulder at 1719 cm^{-1} has been attributed to the carbonyl group formed by the irreversible overoxidation of the thiophene ring in the conducting polymer (CP),[26,46,47] which is induced by the APS. The loading of the peptides during the polymerization process did not affect the bands localization, even though an increase of the band at 1650 cm^{-1} was appreciated due to the presence of peptide bonds. The difference in absolute value between the bands at 1351 cm^{-1} (contribution from PEDOT) and 1650 cm^{-1} (contribution from both the peptide and PEDOT) divided between the maximum minus the minimum of the FTIR spectra expressed in percentage allowed us to compare the different samples. The difference between bands was much more pronounced for PEDOT NPs (98.5%) than for CREKA/PEDOT and CR(*N*Me)EDOT/PEDOT NPs (57.7% and 34.2%, respectively).

To further confirm the successful loading of the peptides, CREKA/PEDOT and CR(*N*Me)EKA/PEDOT NPs were incubated in a Proteinase K solution at 37 ºC for 24 h. Proteinase K is non-specific enzyme with broad cleavage specificity (*i.e.* it cleaves amide bonds adjacent to aliphatic, aromatic or hydrophobic residues).[48] Figure 2b shows the FTIR spectra recorded for digested samples once they were centrifuged, washed three times and dried. The difference between the bands at 1351 and 1650 cm^{-1}, which

was calculated as described above, increased again to 75.4% and 57.7% for CREKA/PEDOT and CR(*N*Me)EKA/PEDOT NPs, respectively, demonstrating the loading of the peptides.

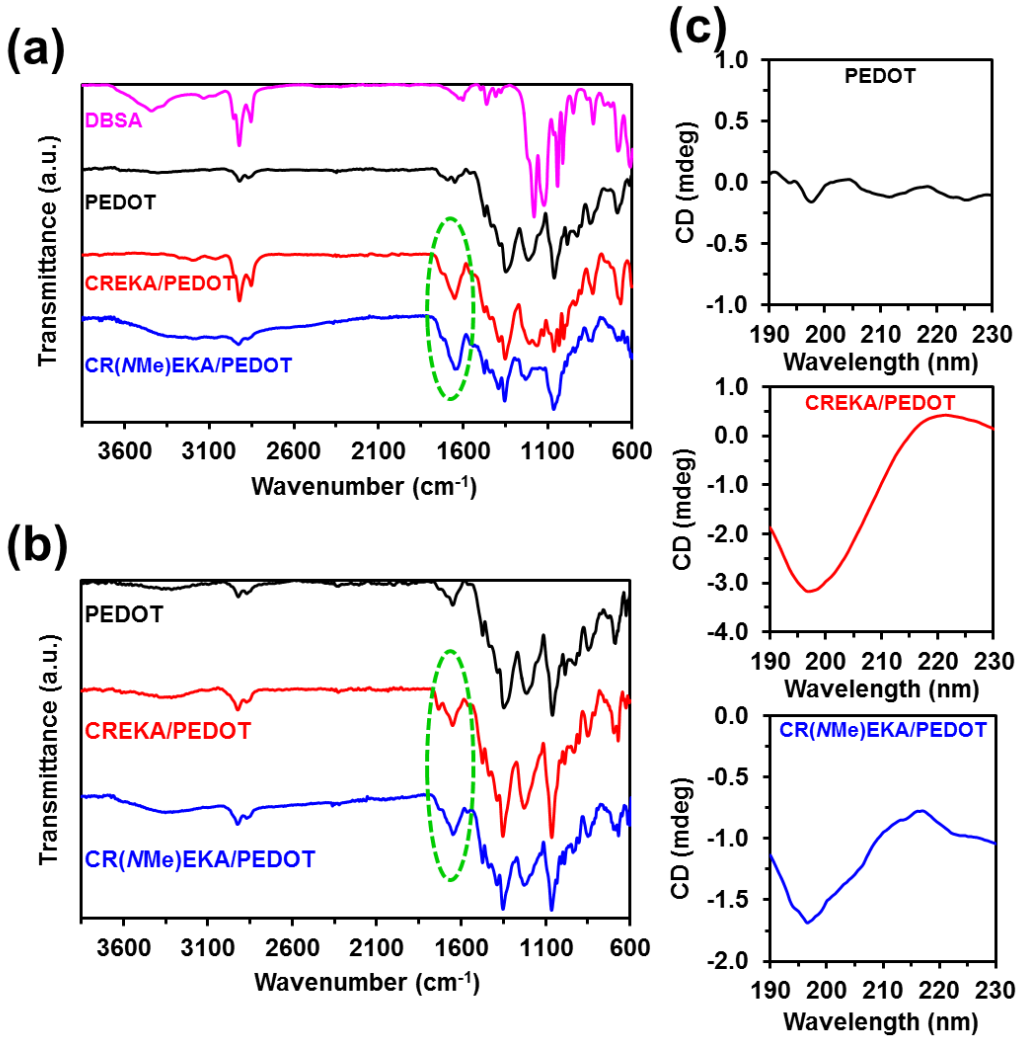

Figure 2. FTIR spectra of DBSA, PEDOT NPs, CREKA/PEDOT NPs and CR(*N*Me)EKA/PEDOT NPs before (a) and after (b) Proteinase K digestion. (c) CD spectra of PEDOT, CREKA/PEDOT and CR(*N*Me)EKA/PEDOT NPs dispersions.

The structure of the loaded peptides was investigated by circular dichroism (CD). The spectrum recorded for PEDOT NPs (Figure 2c) did not show any secondary structure since no chiral compound was in the dispersion. In contrast, the CD spectra

obtained for both CREKA/PEDOT and CR(*N*Me)EKA/PEDOT NPs show a minimum at 197 nm (Figure 2c), which is characteristic of a random coil secondary structure.[49]

In order to examine the effect of the NPs on the stability of CR(*N*Me)EKA, which was engineered to be higher than that of CREKA without loss biological activitity,[11] unloaded (control) and loaded PEDOT NPs (1 mg/mL) where incubated with Proteinase K solution (1.8 U/mL) during 1, 24 and 96 h. Subsequently, the samples were frozen, lyophilized and re-solubilized with loading buffer to run a SDS-PAGE gel. As expected, no peptide band was observed for the control (Figure S1). However, a small band coming from the peptide signal was visualized below 6.5 KDa for CREKA/PEDOT and CR(*N*Me)EKA/PEDOT (Figure S1). The intensity of the band at each time point was compared to the band observed in loaded PEDOT NPs without being incubated with Proteinase K (Figure 3). As observed, the peptide signal lasted longer at higher intensity in the case of CR(*N*Me)EKA/PEDOT NPs, indicating that it needs longer time to be digested by Proteinase K and demonstrating that loaded CR(*N*Me)EKA is more stable than loaded CREKA.

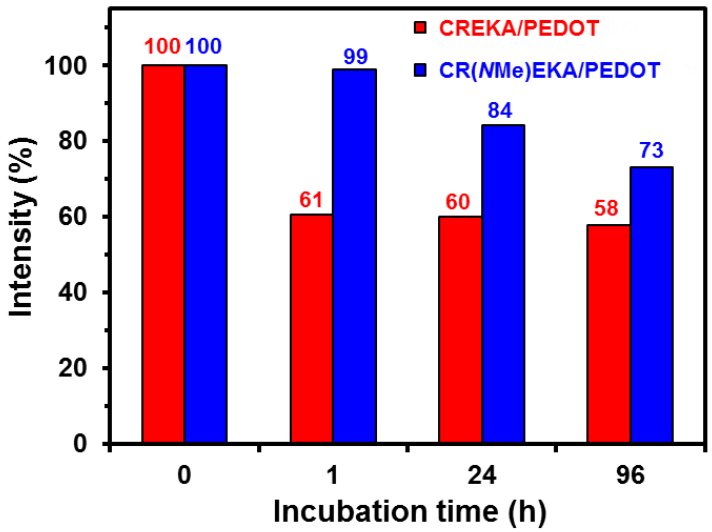

Figure 3. Intensity ratio (from SDS-PAGE gel in Figure S1) for CREKA/PEDOT and CR(*N*Me)EKA/PEDOT NPs before and after being incubated with proteinase K during different periods of time.

The peptide encapsulation efficiency was quantified by HPLC, subtracting the peptide remaining in the supernatant from the total amount of peptide added to the reaction solution. The loading capacity of PEDOT films prepared by anodic polymerization using CREKA and CR(*N*Me)EKA as dopant agents was found to be low (*i.e.* at a ratio of one peptide molecule every ~10 and ~15 polymer repeat units, respectively).[28,29] However, the encapsulation efficiency of PEDOT NPs prepared by emulsion polymerization is significantly higher, as shown in Figure S2. Thus, the amount of encapsulated peptide detected by HPLC was 33.8±4.3 wt% for CREKA and 43.2±2.9 wt% for CR(*N*Me)EKA (*i.e.* one peptide molecule every ~8 and ~6 polymer repeat units, respectively). The amount of encapsulated peptide is expected to be related with the size and amount of the NPs. As shown in Figure 1, the emulsion polymerization used in this work produced a large number of NPs with high surface / volume ratio, enhancing the peptide incorporation with respect to micrometric PEDOT films.

All samples appeared to be spherical, highly monodisperse in size and stable in solution, which is due to the fact that the polymerization process employed in this work was designed to have control on both size and colloidal stability.[26,45] A key criterion for the use of NPs in biomedical applications is the ability to maintain the size of the NPs or their aggregates as small as possible, preventing a blockage in the blood vessels or being eliminated by the body's reticuloendothelial system (RES). More specifically, their size must be below 4 μm, the smallest diameter of human blood capillaries.[50] Figures 4a and 4b display the UV-vis spectra of CREKA/PEDOT and CR(*N*Me)EKA/PEDOT NPs, respectively, dispersed in phosphate buffer saline solution (PBS) at concentrations ranging from 5 to 50 μg/mL. As is shown by the linear increase of absorbance with the increasing peptide-NPs concentrations,[51] both peptide-containing

NPs were perfectly dispersed in PBS without any macroscopic aggregates. The absence of aggregates is also evidenced in optical microscopy images deposited onto a cover glass (Figure 4c).

The NPs stability was corroborated with dynamic light scattering (DLS) measurements over a period of two weeks (Figure S3). All NPs presented higher diameters than the ones seen by TEM due to the polymer hydration. Nevertheless, this diameter size and polydispersity was maintained during the study (two weeks), presenting some aggregation during the firsts four days for PEDOT and CR(NMe)EKA/PEDOT NPs. Interestingly, NPs with peptides showed smaller diameter than without them. This could mean that peptide presence increases the sample colloidal stability. CREKA/PEDOT NPs presented the smallest diameter and polydispersity.

Hard protein corona on peptide-loaded NPs

In order to achieve targeted delivery systems, it is necessary to evaluate the interaction between the proteins found on body fluids with the designed carriers. When materials are in contact with biological fluids they adsorb different biomolecules due to their high surface free energy. Therefore, the hard protein corona, which is a tightly bound monolayer of proteins with high affinity for the NPs surface, will define the biological identity of engineered NPs, influencing cytotoxicity, targeting, body distribution and endocytosis into specific cells.[52] Although recent advances on this field have been done, not much attention has been focused on CP⋯protein interactions. For that reason, in this section we explore this field using fetal bovine serum (FBS) as a representative mixture of serum proteins. The discussion of this section is focused on the formation of the protein corona on PEDOT, CREKA/PEDOT and

CR(*N*Me)EKA/PEDOT NPs rather than on the detailed composition and properties of such corona.

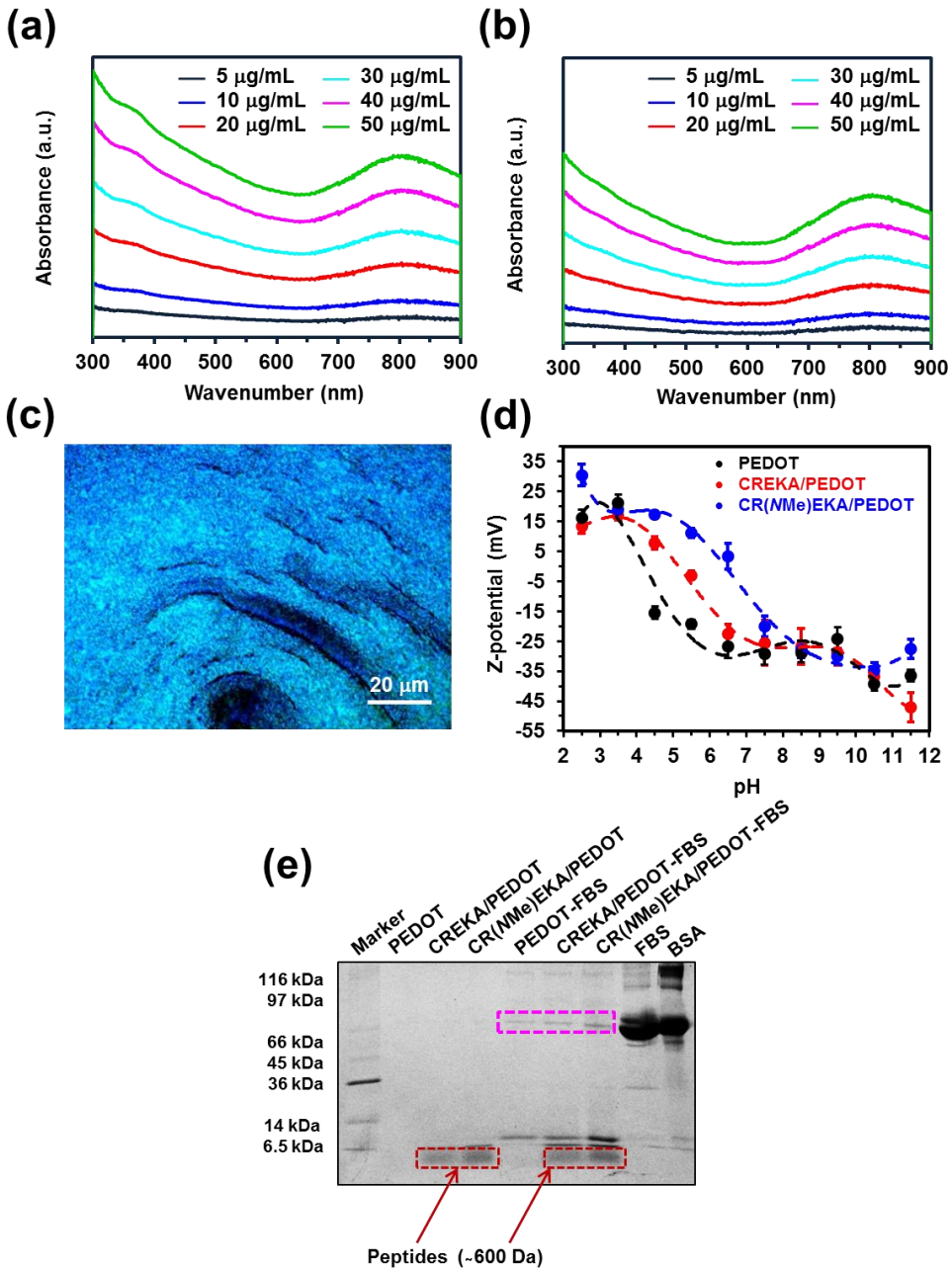

Figure 4. UV-Vis spectra of (a) CREKA/PEDOT and (b) CR(*N*Me)EKA/PEDOT NPs at different concentrations (from 5 to 50 µg/mL). (c) Optical Image of CREKA/PEDOT NPs deposited onto a cover glass. (d) Aqueous electrophoretic curves recorded for PEDOT, CREKA/PEDOT and CR(*N*Me)EKA/PEDOT NPs dispersed in 1 mM KCl at different pHs. (e) SDS-PAGE analysis of the pattern of FBS proteins adsorbed on PEDOT, CREKA/PEDOT and CR(*N*Me)EKA/PEDOT NPs. BSA (66 kDa) was run for comparison.

The variation of the surface Z-potential with the pH was determined for the NPs by aqueous electrophoresis since the charge at the slipping plane is expected to influence protein absorption. Figure 4d shows the electrophoretic curves obtained for re-dispersed PEDOT, CREKA/PEDOT and CR(*N*Me)EKA/PEDOT NPs in the presence of 1 mM KCl as background electrolyte. The isoelectric point (IP) point of PEDOT NPs was ~4 since the anionic surfactant (pKa 2.8) is adsorbed at the NPs surface, balancing the cationic charge of the PEDOT backbone. Instead, the IP of CREKA/PEDOT and CR(*N*Me)EKA/PEDOT NPs is 5.5 and 6.5, respectively, being closer to that of the peptides (IP: 8.5). Thus, Arg and Lys residues display positive charges while Glu (CREKA) and *N*-methyl-Glu (CR(*N*Me)EKA) residues impart a negative charge.

Subsequently, unloaded and peptide-loaded NPs were incubated with FBS at 37 ºC and then washed three-times in order to get rid of the proteins weakly bound to the surface. According to previous studies, which claim that the protein corona is formed over a period of 1 h, the incubation time was set at 1 h.[53,54] Afterwards, SDS-PAGE gels were run (Figure 4e), confirming the formation of the hard corona. The coronal composition was similar for the three types of NPs, BSA being the most prominent protein on the corona of the three species. However, the quantity of bound proteins was higher for CR(*N*Me)EKA/PEDOT NPs, even though in that case the size of the NP is slightly bigger (*i.e.* lower surface / volute ratio), as shown in Figure 1. The amount of adsorbed proteins increases with the size of the molecules, the charge and the hydrophobicity of the particle surface. In addition, hydrophobic interactions have an important effect on protein adsorption, so that dehydration of hydrophobic areas produces an entropy gain that in turn could facilitate protein adsorption.

In relation with protein adhesion capabilities, isolated and known mixtures of different proteins were investigated at different pHs (*i.e.* acid, neutral and basic) for the

three types of NPs. The chosen proteins were lysozyme (LYS; IP= 11.3), bovine serum albumin (BSA; IP= 4.7) and fibrinogen (Fg; IP= 5.5). Gel electrophoresis, which proves the size and charge of a species, simultaneously, and Z-potential of the washed NPs after incubation with LYS, BSA and Fg for 1 h at 37 ºC are displayed in Figure 5.

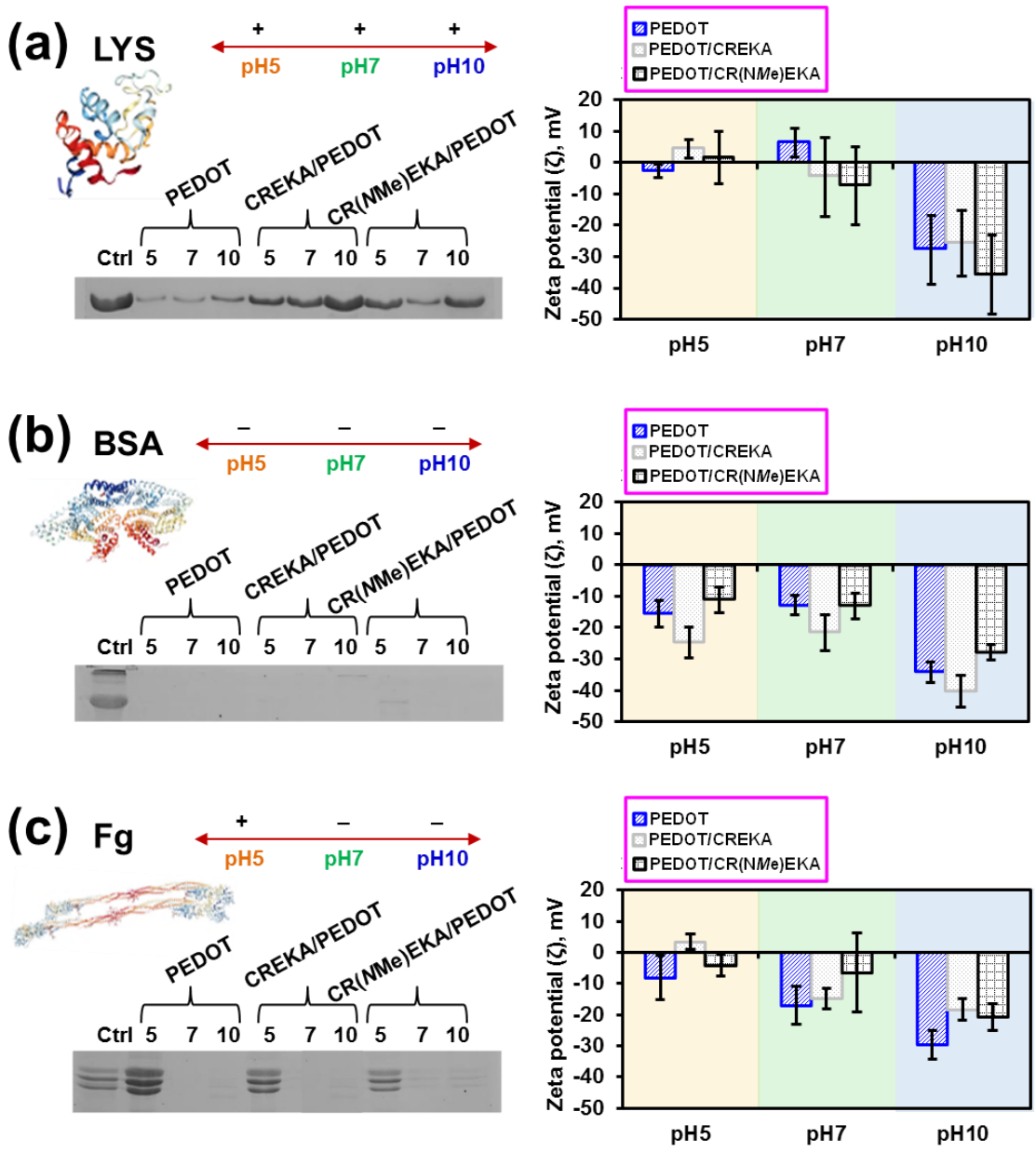

Figure 5. SDS-PAGE (left) and Zeta potential (right) of the PEDOT, CREKA/PEDOT and CR(*N*Me)EKA NPs incubated with (a) LYS, (b) BSA and (c) Fg at different pHs (5, 7, 10).

Importantly, protein···NP complexes were only formed when proteins were positively charged (*i.e.* LYS at the three studied pHs and Fg at pH 5). In Figure 4 it is possible to detect BSA bounded to NPs, however, this is just an indicative that when many proteins are present they can bound to each other generating protein multilayers. For instance, BSA can be bound to positively charged proteins bound to NPs surface. Comparison of the Z-potential of the NPs before (Figure 4d) and after protein incubation (Figure 5) reflects a change in the effective electric charge of peptide loaded NPs surface, which becomes less negative than for unloaded NPs when positively charged proteins are bound. Similar studies were conducted using equimolar LYS:Fg and LYS:BSA mixtures. As shown in Figure S4, after incubation the binding on the NPs was greater for Fg than for BSA. As it was expected, this effect was more pronounced for the peptide-loaded NPs than for the unloaded ones due to the specific affinity of CREKA and CR(NMe)EKA towards Fg.[11,29]

Cytotoxicity and cellular-uptake of peptide-loaded NPs

Previous studies *in vitro* and *in vivo* have demonstrated PEDOT as a biocompatible material.[38,55-57] Also, therapeutic doses of CREKA and CR(*N*Me)EKA were investigated *in vivo*.[11] In this work, the cytotoxicity of DBSA, PEDOT NPs, CREKA/PEDOT and CR(*N*Me)EKA/PEDOT NPs was tested in four different cell lines: metastatic prostate epithelial cells (PC3); Rattus norvegicus kidney normal cells (NRK); Madin-Darby canine kidney (MDCK) cells transfected with the cDNA of human 2,6-sialtransferase (SIAT); normal prostate epithelium immortalized with SV40 (PNT2). The viability of PC3 cells (highest toxicity among the studied cell lines), as determined by the MTT assay, after 24 h post-treatment is compared in Figure 6a for the four materials under study and the corresponding control (cells incubated in the

wells without NPs), while results obtained for NRK, MDCK-SIAT and PNT2 cell lines are shown in Figure S5.

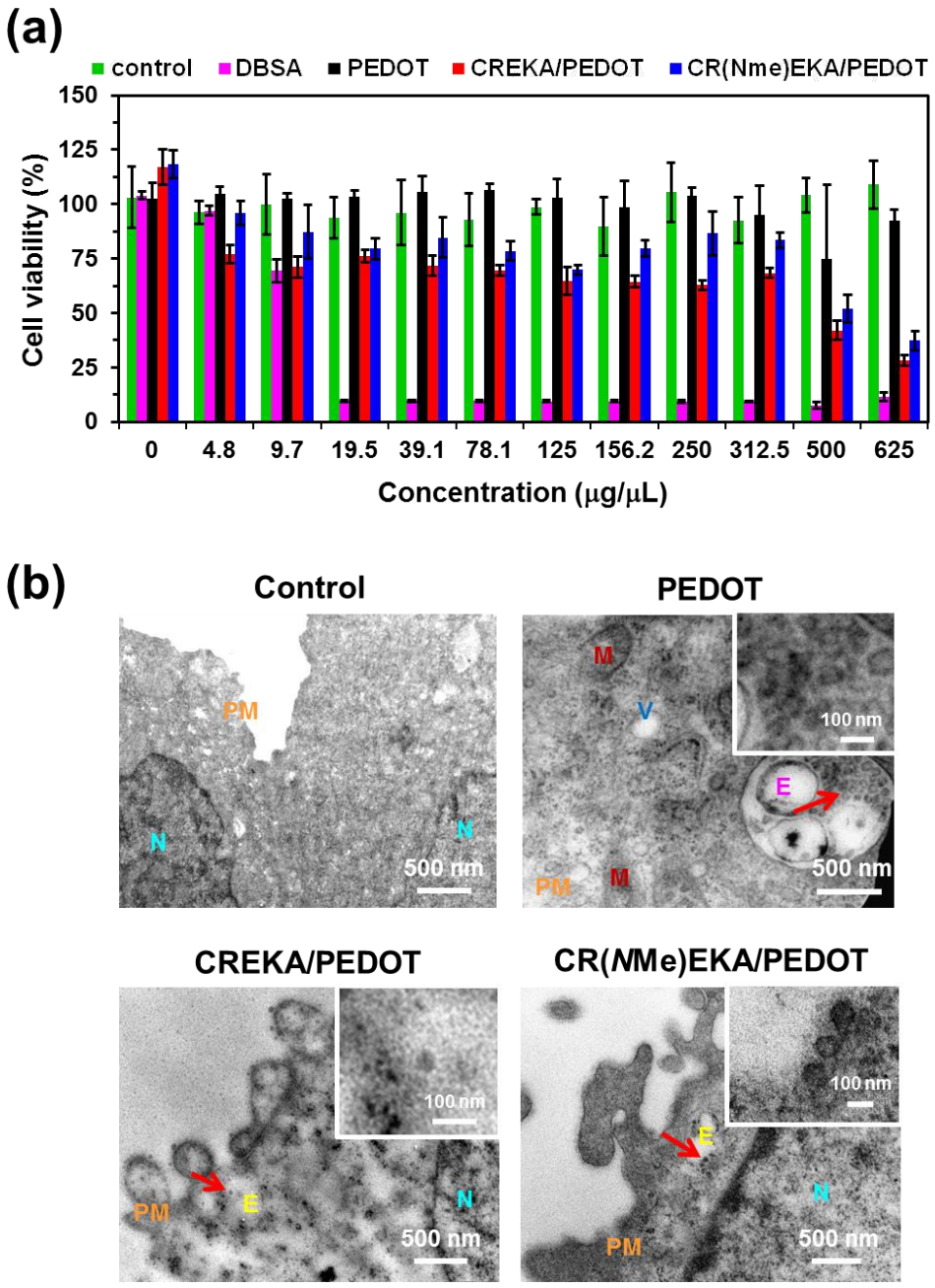

Figure 6. (a) Cytotoxicity studies of PEDOT, CREKA/PEDOT and CR(*N*Me)EKA/PEDOT NPs on PC3 cells for 24 h. For the sake of completeness, independent cytotoxicity studies were also conducted for DBSA. Values are the mean of 3 samples and bars indicate their standard deviation. Results for NRK, MDCK-SIAT and PNT2 cells are displayed in Figure S6. (b) TEM images of PC3 cells incubated without NPs (control), PEDOT NPs (blank), CREKA/PEDOT NPs and

CR(NMe)EKA/PEDOT-CR(NMe)EKA NPs for 24 h (25 mg/mL). Red arrows indicate the NPs. (N: nucleus; M: mitochondria; V: vacuoles; E: endosome; and PM: plasma membrane).

Results indicate that the PEDOT NPs do not exert toxicity on PC3 cells, even at very high concentrations. This has been attributed to the elimination of the DBSA, which was used as stabilizer and dopant agent in the emulsion polymerization process, during the successive washing steps applied after the synthesis of the NPs. Indeed, although the toxic effect of DBSA on PC3 cells starts at ~6 μg/μL, this concentration is around 533 times lower than the one used for the synthesis of PEDOT NPs. Cell viability profiles obtained for NRK, MDCK-SIAT and PNT2 cells provided similar observations with respect to the potential role of PEDOT NPs to act as non-toxic drug carriers and the toxicity of DBSA, even though the latter showed cell line dependence. Thus, the cytotoxicity of DBSA against NRK, MCDK-SIAT and PNT2 cells was 16, 8 and 2 times less severe than its cytotoxicity against PC3 cells.

Peptide-loaded NPs present some differences with respect to the harmless unloaded PEDOT NPs. In general, cell viabilities in PC3 (Figure 6a) are lower for CREKA/PEDOT and CR(*N*Me)DOT/PEDOT than for PEDOT. However, no significant cell death was detected for peptide-loaded NPs as compared to nontoxic unloaded PEDOT until a high NPs concentration was tested (*i.e.* 500 μg/μL). Instead, cell viabilities in NRK, MDCK-SIAT and PNT2 (Figure S5) are comparable (NRK) or even higher (MCDK-SIAT and PNT2) for peptide-loaded NPs than for unloaded NPs, suggesting that the toxicity effects of CREKA and CR(*N*Me)EKA depends significantly on the cell line. Differences between the response of PC3 and the other three cell lines against the peptide concentration might be due to the formation Zn–S interactions involving the sulphur atom of Cys. Although the redox metabolism associated with Zn–

S(Cys) complexes is involved in protein structure regulation,[58] alterations in the Zn^{2+} regulation cause stress, even inducing cellular apoptosis. Considering that proliferation and survival of PC3 cells is known to be very sensitive to free Zn^{+2},[59] it can be hypothesized that Zn-chelation through the formation Zn–S(Cys) complexes explains the effects of the studied peptides in this cell line.

In order to provide a more comprehensive understanding of the response of cells to peptide-loaded NPs exposure, transmission electron microscopy (TEM) was used to study the internalization of the NPs by PC3 cells. This cell line was selected because of its sensitivity to the toxicity effects of CREKA and CR(*N*Me)EKA. Figure 6b shows representative TEM images of PC3 cells incubated in absence of NPs (control) and with PEDOT (blank), CREKA/PEDOT and CR(*N*Me)EDOT/PEDOT NPs for 24 h. Additional TEM micrographs for CREKA/PEDOT and CR(*N*Me)EDOT/PEDOT are provided in Figure S6. The three types of examined NPs were internalized in PC3 cells, even though the uptake process did not induce significant changes in the cell morphology. NPs enter the cell as individual or groups of some few particles and, upon entering the cytoplasm, they form vesicular endosome-like structures. This distribution of the internalized NPs suggests that NPs were taken up by PC3 cells through endocytosis (isolated NPs) and phagocytosis (groups of NPs), which is the uptake for particulates larger than ~0.5 μm. Both processes start through the binding of NPs to specific cell surface proteins and receptors.

Electro-stimulated peptide release

Before conducting electrically stimulated peptide delivery assays, the influence of the CREKA and CR(*N*Me)EKA on the electrochemical activity of PEDOT NPs was examined by cyclic voltammetry. Figure 7a shows the voltammograms recorded for

glassy carbon electrodes coated with PEDOT, CREKA/PEDOT and CR(*N*Me)EKA/PEDOT NPs at different scan rates (*c*) in PBS 1× pH 7.4. As expected, in all cases the current intensity increases with *c*. Moreover, the peptides do not have a significant influence in the electrochemical activity of the CP NPs, the area and shape of the voltammograms being similar for the three systems under study, independently of *c*.

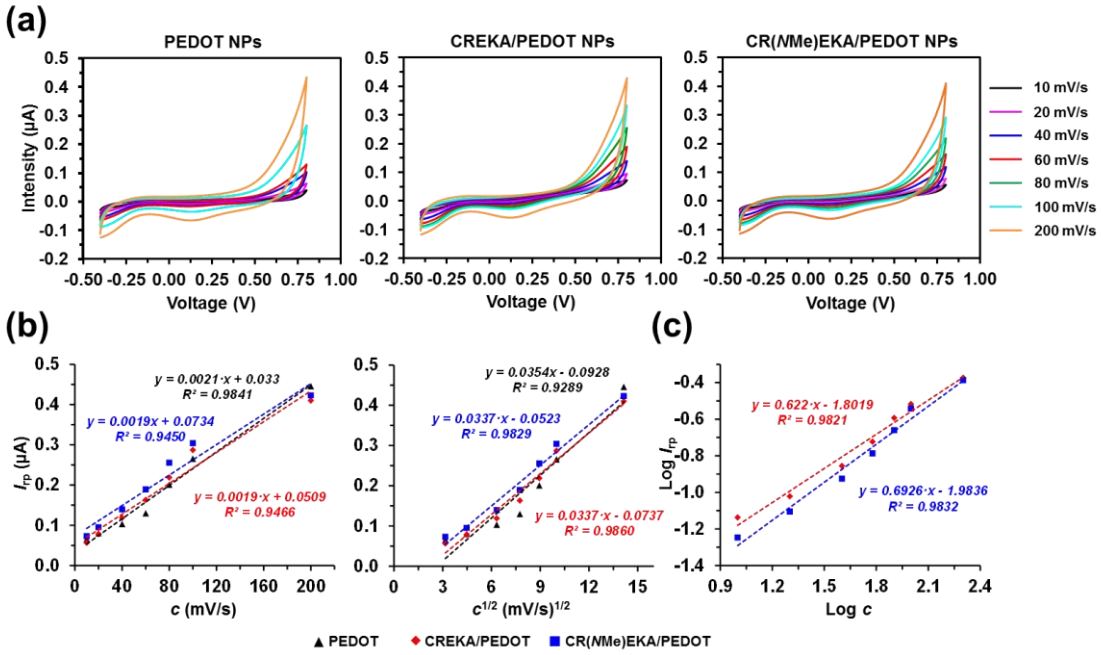

Figure 7. (a) Cyclic voltammograms recorded for glassy carbon electrodes coated with PEDOT, CREKA/PEDOT and CR(*N*Me)EKA/PEDOT NPs at scan rates from 10 to 200 mV/s in PBS 1×. (b) Variation of the intensity at the reversal potential (I_{rp}) *versus* the scan rate (*c*) and square root of the scan rate ($c^{1/2}$) for PEDOT, CREKA/PEDOT and CR(*N*Me)EKA/PEDOT NPs. (c) Logarithm of the intensity at the reversal potential (Log I_{rp}) versus the logarithm of the scan rate (Log *c*) for CREKA/PEDOT and CR(*N*Me)EKA/PEDOT NPs.

The anodic peak (oxidation process) at a potential higher than the reversal potential and the cathodic peak (reduction process) at 0.14 V are well defined in all cases, the corresponding peak current intensity increasing with *c*. Figure 7b compares the variation of the intensity at the reversal potential (I_{rp}) *versus* both *c* and square root of *c*

($c^{1/2}$) for unloaded and peptide-loaded PEDOT NPs (left and right, respectively). For unloaded PEDOT NPs, the highest linearity was obtained for the variation of the intensity against c (R^2= 0.9841), indicating that this system is predominantly controlled by absorption processes. Instead, the linearity of I_{rp} and $c^{1/2}$ was higher for CREKA/PEDOT and CR(NMe)EKA/PEDOT NPs, which indicates that peptide-loading transforms PEDOT NPs into predominantly diffusion controlled current systems. Indeed, although the plot of the logarithm of I_{rp} versus the logarithm of c retains the linear behavior for CREKA/PEDOT and CR(NMe)EKA/PEDOT NPs (Figure 7c), the obtained slopes (0.62 and 0.69, respectively) differ from the theoretical value of 0.5 for an ideal diffusion controlled system,[60] evidencing the participation of absorption processes as in unloaded NPs.

The release of the peptides from loaded NPs was quantified by HPLC at 220 nm in all cases. The released amount of peptide from CREKA/PEDOT NPs triggered by cyclic voltammetry (CV) stimuli in PBS is displayed in Figure 8a. As a control, HPLC chromatograms were taken from CREKA/PEDOT NPs dipped in PBS to which no electrical stimulus was applied. As expected, there was no significant release of CREKA by diffusion after 24 h from those control samples, evidencing that CREKA/PEDOT is an electrically regulated release system. From the initially loaded peptide, 14.4% ± 7.6% and 35.0%±6.6% were released after 50 and 100 CV cycles, respectively, at a scan rate of 100 mV/s. This represents a release of ~0.3% per CV cycle, which could allow an exhaustive control of the dosage.

The fundamental principle behind this release is based on the movement of ions in or out of PEDOT NPs:

$$[(\text{PEDOT}^{\alpha+}\cdot\alpha\text{DBSA}^{-})\cdots n\text{CREKA}^{+} + \beta e^{-}] \leftrightarrow [(\text{PEDOT}^{(\alpha-\beta)+}\cdot(\alpha-\beta)\text{DBSA}^{-}) \cdots m\text{CREKA}^{+} + \beta\cdot\text{DBSA}^{-} + (n-m)\text{CREKA}^{+}] \quad (1)$$

The mechanism expressed in Eqn (1), which is sketched in Scheme 2 for CREKA/PEDOT NPs, shows that, initially, the peptide remains adsorbed onto the NPs through attractive electrostatic interactions between the positively charged residues of the (Arg and Lys) and the dopant $DBSA^-$ anions. After the injection of electrons during the cathodic scan, the doping level (*i.e.* the amount of positive charge distributed along PEDOT chains) decreases and, therefore, some dopant anions are expelled from the NPs surface. This change in the oxidation level of the CP and the consequent reduction of $DBSA^-$ anions affects the electrostatic interactions with peptide, which is partially released to the medium.

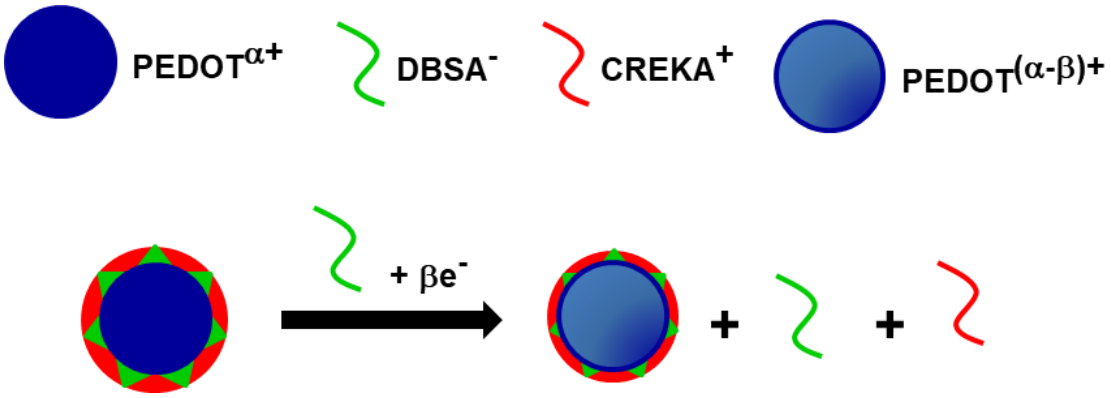

Scheme 2. Sketch illustrating the mechanism of peptide release from CREKA/PEDOT NPs. The change in the intensity of the blue color of the NPs refer to a reduction of the doping level. The reduction of the thickness representing adsorbed $DBSA^-$ and peptide molecules indicate the release of these molecules associated to the decrease of doping level.

In CV assays the potential was swept from a negative potential (-0.40 V) to a positive potential (+0.80 V) changing the oxidation state of the CP NPs supported onto stainless steel, as is reflected by the recorded voltammograms (Figure 8a). The reduction of the PEDOT NPs causes the release the peptide, while ions from the PBS medium are incorporated when the NPs are oxidized.

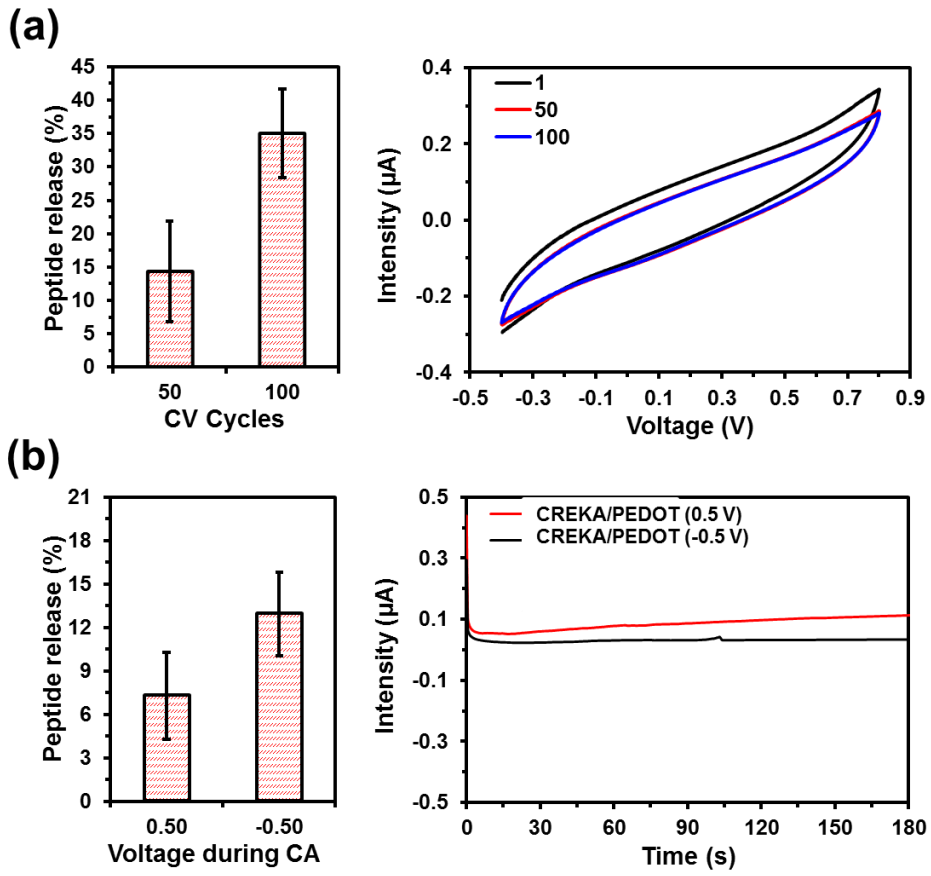

Figure 8. (a) Peptide (in %) released from CREKA/PEDOT NPs by applying 50 and 100 CV cycles at 100 mV/s (left) using a potential window between -0.40 V (initial and final potential) and 0.80 V (reversal potential) and recorded voltammograms (right) for stainless steel coated with CREKA/PEDOT NPs. (b) Peptide (in %) released from CREKA/PEDOT NPs by applying a potential of +0.50 V and -0.50 V during 180 s (left) and recorded chronoamperograms (right) for stainless steel electrode coated with CREKA/PEDOT NPs.

Additional studies were also conducted to monitor the CREKA release from loaded NPs by chronoamperometry (CA) applying voltages of +0.50 and -0.50 V for 180 s. As shown in Figure 8b, the application of the positive potential resulted in a very low release (7.3% ± 3.0%) after such period of time. This expected result has been attributed to the structural damages caused by the overoxidation of the CP, which induces the release of a small fraction of peptide. This phenomenon is reflected in the recorded

chronoamperograms, which display a progressive increment in the current intensity with time. Instead, the application of a negative potential causes the reduction of the CP and the release of 14.9% ± 2.8% of the loaded peptide. The latter value is significantly lower than that obtained using CV, indicating that CA is not the appropriate technique to regulate the pentapeptide release by electrical stimulation.

As it was expected, results for CR(*N*Me)EKA/PEDOT NPs, which are shown in Figure S7, are consistent with those discussed for CREKA/PEDOT. Thus, the peptide release was significantly higher by CV than by CA, reaching a total amount of 16.1% ± 6.2% and 37.8%±6.3% after 50 and 100 CV cycles, respectively.

In order to explore a possible approach to inject CREKA/PEDOT and CR(*N*Me)EDOT/PEDOT NPs *in vivo;* chitosan (CHI) hydrogels containing the NPs were engineered and analyzed by CV. It is worth noting that this system could allow the injection of the NPs through a 3D network of a biocompatible polymer rather than attached to stainless steel electrodes. A similar approach was shown by Ge *et al.*,[32] who loaded polypyrrole NPs in a temperature-sensitive hydrogel that was subsequently used for *in vivo* controlled drug delivery. In the present work, 10 µL of CHI hydrogel alone and CHI loaded with PEDOT, CREKA/PEDOT and CR(*N*Me)EKA/PEDOT NPs (CHI-PEDOT, CHI-CREKA/PEDOT and CHI-CR(*N*Me)EDOT, respectively) were dropped on screen printed electrodes (Figure 9a). Cyclic voltammograms, which were recorded at 100 mV/s from -0.4V to 0.8V, are displayed in Figure 9b and are similar to the ones obtained using NPs directly supported onto solid electrodes (Figure 7a). Indeed, current densities are higher for CP NPs loaded into hydrogels than for CP NPs supported on solid electrodes. This feature indicates that CHI hydrogels allow a more efficient electron transfer between the electrolytic solution and the CP NPs than solid electrodes, which has been attributed to the greater accessibility of the NPs loaded into the

hydrogel. Overall, these results demonstrate that the combination of CP NPs and CHI hydrogels could be used to deliver therapeutic peptides.

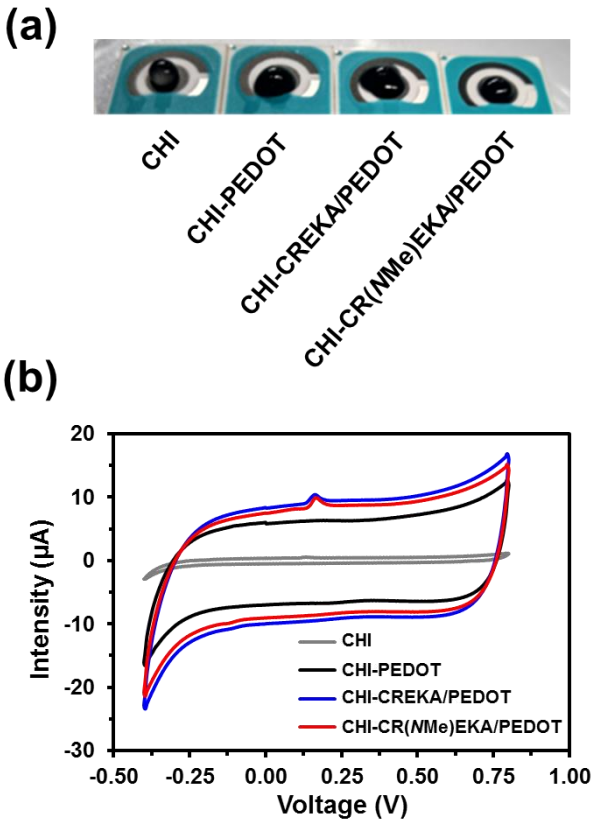

Figure 9. (a) Photographs of unloaded CHI hydrogel and loaded CHI-PEDOT, CHI-CREKA/PEDOT and CHI-CR(*N*Me)EKA/PEDOT hydrogels drop-casted onto screen printed electrodes. (b) Cyclic voltammograms of CHI alone, CHI-PEDOT, CHI-CREKA/PEDOT and CHI-CR(*N*Me)EKA/PEDOT in PBS 1×, pH 7.4.

Considering previous *in vivo* studies using electroresponsive drug-loaded NPs embedded in biodegradable hydrogels,[32] which showed the absence of fibrous tissue encapsulation and excellent biocompatibility, and the benefits observed in this work for PEDOT NPs loaded with CREKA and CR(*N*Me)EKA, our next step for the biomedical application of these CREKA/PEDOT and CR(*N*Me)EKA/PEDOT NPs as drug delivery systems will be the incorporation of the biodegradable groups. More specifically, NPs will be prepared using macromonomers formed by small PEDOT tracts ended with

enzymatically cleavable or hydrolysable linkages (*e.g.* esters).[61] This strategy has been successfully used for the preparation of conductive films for other biomedical applications.[62,63]

CONCLUSIONS

CREKA and CR(*N*Me)EKA can be easily incorporated onto PEDOT NPs and released in a controlled manner depending on the applied *stimuli*. Analyses of the interaction between PEDOT NPs and biological fluids indicates that the protein corona is mainly governed by electrostatic forces between the NP surface and the protein charge, which is completely dependent on the solution pH. Although the therapeutic applications of CREKA are not within the scope of this work because they have been extensively demonstrated,[1-19,28,29] our results evidence that PC3 cells are more susceptible to CREKA and CR(*N*Me)KA loaded particles than MCDK-SIAT, NRK and PNT2 cells. The release of CREKA and CR(*N*Me)EKA can be fine-tuned by modulating the strength of peptide···CP interactions, which becomes weaker when polymer chains are reduced and oxidized applying an external voltage. Two different types of electrical stimuli have been compared: fixed voltage *vs* voltage linear ramp, being the latter much more effective than the former. Peptide ~0.3% release was achieved every CV cycle.

It should be mentioned that PEDOT, as many other CPs, is not itself inherently biodegradable, however, resorbable versions of this CP are currently under development by adding enzymatically cleavable or hydrolysable linkages as connections between small segment with electronic conductivity. As loaded PEDOT NPs have been revealed as a promising complement for CREKA and CR(*N*Me)EKA-based therapeutics, we are

currently working in development of biodegradable PEDOT-based NPs for this biomedical application.

ACKNOWLEDGEMENTS

Authors acknowledge received funding from MINECO/FEDER (RTI2018-098951-B-I00), the Agència de Gestió d'Ajuts Universitaris i de Recerca (2017SGR359) and B. Braun Surgical S.A. company. Funding support for the research of C.A. was received through the prize "ICREA Academia" for excellence in research through the Generalitat de Catalunya.

SUPPORTING INFORMATION

The Supporting Information is available free of charge on the ACS Publications website at DOI:XXXXX. Description of the experimental methods, results from HPLC, SDS-PAGE and cytotoxicity studies, additional TEM micrographs and peptide release from CR(*N*Me)EKA/PEDOT NPs.

REFERENCES

1. Zhang, B; Wang, H; Shen, S.; She, X.; Shi, W.; Chen, J.; Zhang, Q.; Hu, Y.; Pang, Z.; Jiang, X. Fibrin-Targeting Peptide CREKA-Conjugated Multi-Walled Carbon Nanotubes for Self-Amplified Photothermal Therapy of Tumor. *Biomaterials* **2016**, *79*, 46–55. DOI: 10.1016/j.biomaterials.2015.11.061
2. Chung, E. J.; Cheng, Y.; Morshed, R.; Nord, K.; Han, Y.; Wegscheid, M. L.; Auffinger, B.; Wainwright, D. A.; Lesniak, M. S.; Tirrell, M. V. Fibrin-Binding, Peptide Amphiphile Micelles for Targeting Glioblastoma. *Biomaterials* **2014**, *35*, 1249–1256. DOI: 10.1016/j.biomaterials.2013.10.064

3. Puiggalí-Jou, A.; del Valle, L. J.; Armelin, E.; Alemán, C. Fibrin Association at Hybrid Biointerfaces Made of Clot-Binding Peptides and Polythiophene. *Macromol. Biosci.* **2016**, *16*, 1461–1474. DOI: 10.1002/mabi.201600128
4. Simberg, D.; Duza, T.; Park, J. H.; Essler, M.; Pilch, J.; Zhang, L.; Derfus, A. M.; Yang, M.; Hoffman, R. M.; Bhatia, S.; Sailor, M. J.; Ruoslahti, E. Biomimetic Amplification of Nanoparticle Homing to Tumors. *Proc. Natl. Acad. Sci. U. S. A.* **2007**, *104*, 932–936. DOI: 10.1073/pnas.0610298104
5. Zhou, Z.; Wu, X.; Kresak, A.; Griswold, M.; Lu, Z. R. Peptide Targeted Tripod Macrocyclic Gd(III) Chelates for Cancer Molecular MRI. *Biomaterials* **2013**, *34*, :7683–7693. DOI: 10.1016/j.biomaterials.2013.06.057
6. Song, Y.; Huang, Z.; Xu, J.; Ren, D.; Wang, Y.; Zheng, X.; Shen, Y.; Wang, L.; Gao, H.; Hou, J.; Pang, Z.; Qian, J.; Ge, J. Multimodal SPION-CREKA Peptide Based Agents for Molecular Imaging of Microthrombus in a Rat Myocardial Ischemia-Reperfusion Model. *Biomaterials* **2014**, *35*, 2961–2970. DOI: 10.1016/j.biomaterials.2013.12.038
7. Zeng, Z.; Chen, Z.; Tang, L.; Yang, H.; Liu, N.; Zhou, H.; Li, Y.; Wu, J.; Deng, Z.; Deng, H.; Hong, X.; Xiao, Y. A Novel Near-Infrared Fluorescent Light-Up Probe for Tumor Imaging and Drug-Induced Liver Injury Detection. *Chem. Commun.* **2019**, *55*, 2541–2544. DOI: 10.1039/C8CC10286D
8. Wang, L.-j.; Li, H.-s.; Wang, Q.-s.; Wu, H.-b; Han, Y.-j; Zhou, W.-l; Wang, M.; Huang, S. Construction and Evaluation of the Tumor-Targeting, Cell-Penetrating Multifunctional Molecular Probe iCREKA. *Contrast Media Mol. Imaging* **2018**, *2018*, 7929617. DOI:10.1155/2018/7929617

9. Zhou, Z. X.; Qutaish, M.; Han, Z.; Schur, R. M.; Liu, Y. Q.; Wilson, D. L.; Lu, Z. R. MRI Detection of Breast Cancer Micrometastases with a Fibronectin-Targeting Contrast Agent. *Natur. Commun.* **2015**, *6*, 7984. DOI: 10.1038/ncomms8984
10. Jiang, K.; Song, X.; Yang, L.; Li, L.; Wan, Z.; Sun, X.; Gong, T.; Lin, Q.; Zhang, Z. Enhanced Antitumor and Anti-Metastasis Efficacy Against Aggressive Breast Cancer with a Fibronectin-Targeting Liposomal Doxorubicin *J. Control. Release* **2018**, *271*, 21–30. DOI: 10.1016/j.jconrel.2017.12.026
11. Agemy, L.; Sugahara, K. N.; Kotamraju, V. R.; Gujraty, K.; Girard, O. M.; Kono, Y.; Mattrey, R. F.; Park, J.-H.; Sailor, M. J.; Jimenez, A. I.; Cativiela, C.; Zanuy, D.; Sayago, F. J.; Alemán, C.; Nussinov, R.; Ruoslahti, E. Nanoparticle-Induced Vascular Blockade in Human Prostate Cancer. *Blood* **2010**, *116*, 2847−2856. DOI: 10.1182/blood-2010-03-274258
12. Okur, A. C.; Erkoc, P.; Kizilel, S. Targeting Cancer Cells via Tumor-Homing Peptide CREKA Functional PEG Nanoparticles. *Colloids Surf. B* **2016**, *147*, 191–200. DOI: 10.1016/j.colsurfb.2016.08.005
13. Wu, J.; Zhao, J.; Zhang, B.; Qian, Y.; Gao, H.; Yu, Y.; Wei, Y.; Yang, Z.; Jiang, X.; Pang, Z. Polyethylene Glycol–Polylactic Acid Nanoparticles Modified with Cysteine–Arginine–Glutamic Acid–Lysine–Alanine Fibrin-Homing Peptide for Glioblastoma Therapy by Enhanced Retention Effect. *Int. J. Nanomedicine* **2014**, *9*, 5261–5271. DOI: 10.2147/IJN.S72649
14. Zhao, J.; Zhang, B.; Shen, S.; Chen, J.; Zhang, Q.; Jiang, X.; Pang, Z. CREKA Peptide-Conjugated Dendrimer Nanoparticles for Glioblastoma Multiforme Delivery. *J. Colloid Interf. Sci.* **2015**, *450*, 396–403. DOI: 10.1016/j.jcis.2015.03.019

15. Zhong, Y.; Zhang, Y.; Xie, J.; Zhou, J.; Liu, J.; Ye, M.; Zhang, L.; Qiao, B.; Wang, Z.g.; Ran, H.-t.; Guo, D. Low-Intensity Focused Ultrasound-Responsive Phase-Transitional Nanoparticles for Thrombolysis without Vascular Damage: A Synergistic Nonpharmaceutical Strategy. *ACS Nano* **2019**, *13*, 3387−3403. DOI: 10.1021/acsnano.8b09277
16. Perera, V. S.; Covarrubias, G.; Lorkowski, M.; Atukorale, P.; Rao, A.; Raghunathan, S.; Gopalakrishnan, R.; Erokwu, B. O.; Liu, Y.; Dixit, D.; Brady-Kalnay, S. M.; Wilson, D.; Flask, C.; Rich, J.; Peiris, P. M.; Karathanasis, E. One-Pot Synthesis of Nanochain Particles for Targeting Brain Tumors. *Nanoscale* **2017**, *9*, 9659–9667. DOI: 10.1039/c7nr02370g
17. Poon, C.; Gallo, J.; Joo, J.; Chang, T.; Banobre-Lopez, M.; Chung, E. J. Hybrid, Metal Oxide‑Peptide Amphiphile Micelles for Molecular Magnetic Resonance Imaging of Aterosclerosis. *J. Nanobiotechnol.* **2018**, *16*, 92. DOI: 10.1186/s12951-018-0420-8
18. de Oliveira Freitas, L. B.; de Melo Corgosinho, L.; Arantes Faria, J. A. Q.; dos Santos, V. M.; Resende, J. M.; Leal, A. S.; Gomes, D. A.; Barros de Sousa, E. M. Multifunctional Mesoporous Silica Nanoparticles for Cancer-Targeted, Controlled Drug Delivery and Imaging. *Microporous Mesoporous Mater.* **2017**, *242*, 271–283. DOI: 10.1016/j.micromeso.2017.01.036
19. Kruse, A. M.; Meenach, S. A.; Anderson, K. W.; Hilt, J. Z. Synthesis and Characterization of CREKA-Conjugated Iron Oxide Nanoparticles for Hyperthermia Applications. *Acta Biomater.* **2014**, *10*, 2622–2629. DOI: 10.1016/j.actbio.2014.01.025

20. Zanuy, D.; Flores-Ortega, A.; Casanovas, J.; Curcó, D.; Nussinov, R.; Alemán, C. The Energy Landscape of a Selective Tumor-Homing Pentapeptide. *J. Phys. Chem. B* **2008**, *112*, 8692–8700. DOI: 10.1021/jp711477k

21. Curcó, D.; Revilla-López, G.; Alemán, C.; Zanuy, D. Atomistic Modeling of Peptides Bound to a Chemically Active Surface: Conformational implications. *J. Pept. Sci.* **2011**, *17*, 132–138. DOI: 10.1002/psc.1321

22. Curcó, D.; Zanuy, D.; Nussinov, R.; Alemán, C. A Simulation Strategy for the Atomistic Modeling of Flexible Molecules Covalently Tethered to Rigid Surfaces: Application to Peptides. *J. Comput. Chem.* **2011**, *32*, 607–619. DOI: 10.1002/jcc.21647

23. Tandon, B.; Magaz, A.; Balint, R.; Blaker, J. J.; Cartmell, S. H. Electroactive Biomaterials: Vehicles for Controlled Delivery of Therapeutic Agents for Drug Delivery and Tissue Regeneration. *Adv. Drug Deliv. Rev.* **2018**, *129*, 148–168. DOI: 10.1016/j.addr.2017.12.012

24. Puiggalí-Jou, A.; del Valle, L. J.; Alemán, C. Drug Delivery Systems Based on Intrinsically Conducting Polymers. *J. Control. Release.* **2019**, *309*, 244–264. DOI: 10.1016/j.jconrel.2019.07.035

25. Pérez-Madrigal, M. M.; Llorens, E.; del Valle, L. J.; Puiggalí, J.; Armelin, E.; Alemán, C., Semiconducting, Biodegradable and Bioactive Fibers for Drug Delivery. *Express Polym. Lett.* **2016**, *10*, 628–646. DOI: 10.3144/expresspolymlett.2016.58

26. Puiggalí-Jou, A.; Micheletti, P.; Estrany, F.; del Valle, L. J.; Alemán, C. Electrostimulated Release of Neutral Drugs from Polythiophene Nanoparticles: Smart Regulation of Drug-Polymer Interactions. *Adv. Health. Mater.* **2017**, *6*, 1700453. DOI: 10.1002/adhm.201700453

27. Puiggalí-Jou, A.; Cejudo, A.; del Valle, L. J.; Alemán C. Smart Drug Delivery from Electrospun Fibers through Electroresponsive Polymeric Nanoparticles. *ACS Appl. Bio Mater.* **2018**, *1*, 1594–1605. DOI: 10.1021/acsabm.8b00459

28. Fabregat, G.; Teixeira-Dias, B.; del Valle, L. J.; Armelin, E.; Estrany, F.; Alemán, C. Incorporation of a Clot-Binding Peptide into Polythiophene: Properties of Composites for Biomedical Applications. *ACS Appl. Mater. Interfaces* **2014**, *6*, 11940−11954. DOI: 10.1021/am503904h

29. Puiggalí, A.; del Valle, L. J.; Armelin, E.; Alemán, C. Fibrin Association at Hybrid Biointerfaces Madeof Clot-Binding Peptides and Polythiophene. *Macromol. Biosci.* **2016**, *16*, 1461−1474. DOI: 10.1002/mabi.201600128

30. Nezakati, T.; Seifalian, A.; Tan, A.; Seifalian, A. M. Conductive Polymers: Opportunities and Challenges in Biomedical Applications. *Chem. Rev.* **2018**, *14*, 6766–6843. DOI: 10.1021/acs.chemrev.6b00275

31. Boehler, C.; Kleber, C.; Martini, N.; Xie, Y.; Dryg, I.; Stieglitz, T.; Hofmann, U. G.; Asplund, M. Actively Controlled Release of Dexamethasone from Neural Microelectrodes in a Chronic In Vivo Study. *Biomaterials* **2017**, *129*, 176–187. DOI: 10.1016/j.biomaterials.2017.03.019

32. Ge, J.; Neofytou, E.; Cahill, T. J.; Beygui, R. E.; Zare, R. N. Drug Release from Electric Field-Responsive Nanoparticles. *ACS Nano* **2012**, *6*, 227–233. DOI: 10.1021/nn203430m

33. Hsiao, P. F.; Anbazhagan, R.; Tsai, H.-C.; Krishnamoorthi, R.; Lin, S.-J.; Lin, S.-Y; Lee, K.-Y.; Kao, C.-Y.; Chen, R.-S.; Lai, J.-Y. Fabrication of Electroactive Polypyrrole-Tungsten Disulfide Nanocomposite for Enhanced In Vivo Drug Release in Mice Skin. *Mat. Sci. Eng. C-Mater.* **2020**, *107*, 110330. DOI: 10.1016/j.msec.2019.110330.

34. Bubnova, O.; Khan, Z. U.; Wang, H.; Braun, S.; Evans, D. R.; Fabretto, M.; Hojati-Talemi, P.; Dagnelund, D.; Arlin, J. B.; Geerts, Y. H.; Desbief, S.; Breiby, D. W.; Andreasen, J. W.; Lazzaroni, R.; Chen, W. M.; Zozoulenko, I.; Fahlman, M.; Murphy, P. J.; Berggren, M.; Crispin, X. Semi-Metallic Polymers. *Nat. Mater.* **2014**, *13*, 190−194. DOI: 10.1038/nmat3824.

35. Kayser, L. V.; Lipomi, D. J. Stretchable Conductive Polymers and Composites Based on PEDOT and PEDOT:PSS. Integration of Biorecognition Elements on PEDOT Platforms through Supramolecular Interactions. *Adv. Mater.* **2019**, *31*, 1806133. DOI: 10.1002/adma.201806133

36. Sappia, L. D.; Piccinini, E.; Marmisolle, W.; Santilli, N.; Maza, E.; Moya, S.; Battaglini, F.; Madrid, R. E.; Azzaroni, O. Integration of Biorecognition Elements on PEDOT Platforms through Supramolecular Interactions. *Adv. Mater. Interf.* **2017**, *17*, 1700502. DOI: 10.1002/admi.201700502

37. Groenendaal, L. B.; Jonas, F.; Freitag, D.; Pielartzik, H.; Reynolds, J. R. Poly(3,4-ethylenedioxythiophene) and Its Derivatives: Past, Present, and Future. *Adv. Mater.* **2000**, *12*, 481−494. DOI: 10.1002/(SICI)1521-4095(200004)12:7<481::AID-ADMA481>3.0.CO;2-C

38. del Valle, L. J.; Estrany, F.; Armelin, E.; Oliver, R.; Alemán, C.. Cellular Adhesion, Proliferation and Viability on Conducting Polymer Substrates. *Macromol Biosci.* **2008**, *8*, 1144−1151. DOI: 10.1002/mabi.200800101

39. Marti, M.; Fabregat, G.; Estrany, F.; Aleman, C.; Armelin, E. Nanostructured Conducting Polymer for Dopamine Detection. *J. Mater. Chem.* **2010**, *20*, 10652–10660. DOI: 10.1039/C0JM01364A

40. Han, M. G.; Foulger, S. H. Preparation of Poly(3,4-ethylenedioxythiophene)(PEDOT) Coated Silica Core-Shell Particles and PEDOT Hollow Particles. *Chem. Commun.* **2004**, 2154–2155. DOI: 10.1039/b409396h
41. Khan, M. A.; Armes, S. P. Synthesis and Characterization of Micrometer-Sized Poly(3,4 ethylenedioxythiophene)-Coated Polystyrene Latexes. *Langmuir* **1999**, *15*, 3469–3475. DOI: 10.1021/la9815897
42. Luo, S. C.; Yu, H. H.; Wan, A. C. A; Han, Y.; Ying, J. Y. A General Synthesis for PEDOT-Coated Nonconductive Materials and PEDOT Hollow Particles by Aqueous Chemical Polymerization. *Small* **2008**, 4, 2051–2058. DOI: 10.1002/smll.200800033
43. Kelly, T. L.; Wolf, M. O. Template Approaches to Conjugated Polymer Micro- and Nanoparticles. *Chem. Soc. Rev.* **2010**, *39*, 1526–1535. DOI: 10.1039/B914333P
44. Liu, D.; Ma, L.; An, Y.; Li, Y.; Liu, Y; Wang, L.; Guo, J.; Wang, J.; Zhou, J. Thermoresponsive Nanogel-Encapsulated PEDOT and HSP70 Inhibitor for Improving the Depth of the Photothermal Therapeutic Effect. *Adv. Funct. Mater.* **2016**, *26*, 4749–4759. DOI:10.1002/adfm.201600031
45. Li, L.; Liu, Y.; Hao, P.; Wang, Z.; Fu, L.; Ma, Z. PEDOT Nanocomposites Mediated Dual-Modal Photodynamic and Photothermal Targeted Sterilization in Both NIR I and II Window. *Biomaterials* **2015**, *41*, 132–140. DOI: 10.1016/j.biomaterials.2014.10.075
46. Zykwinska, A.; Domagala, W.; Pilawa, B.; Lapkowski, M. Electrochemical Overoxidation of Poly(3,4-ethylenedioxythiophene)—PEDOT Studied by Means of in situ ESR Spectroelectrochemistry. *Electrochim. Acta* **2005**, *50*, 1625-1633. DOI: 10.1016/j.electacta.2004.10.026

47. Tehrani, P.; Kanciurzewska, A.; Crispin, X.; Robinson, N. D.; Fahlman, M.; Berggren, M. The Effect of pH on the Electrochemical Over-Oxidation in PEDOT:PSS Films. *Solid State Ion.* **2007**, *177*, 3521−3527. DOI: 10.1016/j.ssi.2006.10.008

48. Naidoo, A.; Naidoo, K.; Yende-zuma, N.; Gengiah, T. N. Impact of Silk Biomaterial Structure on Proteolysis. *Acta Biomater.* **2015**, *19***,** 161–169. DOI: 10.1016/j.actbio.2014.09.013

49. Matmor, M.; Ashkenasy, N. Peptide Directed Growth Of Gold Films. *J. Mater. Chem.* **2011**, *21***,** 968–974. DOI: 10.1039/C0JM02343D

50. Neuberger, T.; Schöpf, B.; Hofmann, H.; Hofmann, M.; Von Rechenberg, B. Superparamagnetic Nanoparticles for Biomedical Applications: Possibilities and Limitations of a New Drug Delivery System. *J. Magn. Magn. Mater.* **2005**, *293*, 483–496. DOI: 10.1016/j.jmmm.2005.01.064

51. Zha, Z.; Yue, X.; Ren, Q.; Dai, Z. Uniform Polypyrrole Nanoparticles with High Photothermal Conversion Efficiency for Photothermal Ablation of Cancer Cells. *Adv. Mater.* **2013**, *25*, 777–782. DOI: 10.1002/adma.201202211

52. Schöttler, S.; Klein, K.; Landfester, K.; Mailänder, V. Protein Source and Choice of Anticoagulant Decisively Affect Nanoparticle Protein Corona and Cellular Uptake. *Nanoscale* **2016**, *14*, 5526–5536. DOI: 10.1039/c5nr08196c

53. Ritz, S.; Schötter, S.; Kotman, N.; Baier, G.; Kuharev, J.; Landfester, K.; Schild, H.; Jahn, O.; Tenzer, S.; Mailänder, V. Protein Corona of Nanoparticles: Distinct Proteins Regulate the Cellular Uptake. *Biomacromolecules* **2015**, *16*, 1311–1321. DOI: 10.1021/acs.biomac.5b00108

54. Walczyk, D.; Bombelli, F. B.; Monopoli, M. P.; Lynch, I.; Dawson, K. A. What the Cell "Sees" in Bionanoscience. *J. Am. Chem. Soc.* **2010**, *132*, 5761–5768. DOI: 10.1021/ja910675v

55. Stritesky, S.; Markova, A.; Vitecek, J.; Safarikova, E.; Hrabal, M.; Kubac, L.; Kubala, L.; Weiter, M.; Vala, M. Printing Inks of Electroactive Polymer PEDOT:PSS: The Study of Biocompatibility, Stability, and Electrical Properties. *J. Biomed. Mater. Res., Part A* **2018**, *106*, 1121–1128. DOI: 10.1002/jbm.a.36314

56. Bodart, C.; Rosseti, N.; Hagler, J.; Chevreau, P.; Chhin, D.; Soavi, F.; Schougaard, S. B.; Amzica, F.; Cicoira, F. Electropolymerized Poly(3,4-ethylenedioxythiophene) (PEDOT) Coatings for Implantable Deep-Brain-Stimulating Microelectrodes. *ACS Appl. Mater. Interfaces* **2019**, *11*, 17226−17233. DOI: 10.1021/acsami.9b03088.

57. Luo, S.; Ali, E. M.; Tansil, N. C.; Yu, H.; Gao, S.; Kantchev, E. A. B.; Ying, J. Thin, Ultrasmooth, and Functionalized PEDOT Films with in Vitro and in Vivo Biocompatibility. *Langmuir* **2008**, *24*, 8071−8077. DOI: 10.1021/la800333g

58. Maret, W. Zinc and Sulfur: A Critical Biological Partnership. *Biochemistry* **2004**, *43*, 3301–3309. DOI: 10.1021/bi036340p

59. Wetherell, D.; Baldwin, G. S.; Shulkes, A.; Bolton, D.; Ichia J.; Patel, O. Zinc Ion Dyshomeostasis Increases Resistance of Prostate Cancer Cells to Oxidative Stress via Upregulation of HIF1α. *Oncotarget* **2018**, *9*, 8463–8477. DOI: 10.18632/oncotarget.23893

60. Wang, J. Analytical Electrochemistry. Second edition, New York: Wiley-VCH, 2000, p. 37.

61. Da Silva, A. C.; Higgins, M. J.; Cordoba de Torresi, S. I. The effect of nanoscale surface electrical properties of partially biodegradable PEDOT-co-PDLLA

conducting polymers on protein adhesion investigated by atomic force microscopy. *Mater. Sci. Eng. C-Mater.* **2019**, *99*, 468–478. DOI: 10.1016/j.msec.2019.01.103.

62. Molina, B. G.; Cianga, L.; Bendrea, A. D.; Cianga, I.; Alemán, C.; Armelin, E. An Amphiphilic, Heterografted Polythiophene Copolymer Containing Biocompatible/Biodegradable Side Chains for Use As an (Electro)Active Surface in Biomedical Applications. *Polym. Chem.* **2019**, *10*, 5010–5022. DOI: 10.1039/c9py00926d
63. Molina, B. G.; Bendrea, A. D.; Cianga, L.; Armelin, E.; del Valle, L. J;. Cianga, I.; Alemán, C. The Biocompatible Polythiophene-*g*-Polycaprolactone Copolymer As an Efficient Dopamine Sensor Platform. *Polym. Chem.* **2017**, *8*, 6112–6122. DOI: 10.1039/c7py01326d

For Table of Contents Use Only

Title: *Encapsulation and storage of therapeutic fibrin-homing peptides using conducting polymer nanoparticles for programmed release by electrical stimulation*

Authors: *Anna Puiggalí-Jou, Luis J. del Valle and Carlos Alemán*